NDT&E International 42 (2009) 622–629

Contents lists available at ScienceDirect

NDT&E International

journal homepage: www.elsevier.com/locate/ndteint

On the ultimate sensitivity of nonlinear-modulation method of crack detection

V.Yu. Zaitsev *, L.A. Matveev, A.L. Matveyev

Institute of Applied Physics RAS, 46 Uljanova Street, Nizhny Novgorod 603950, Russia

ARTICLE INFO

Article history:
Received 3 September 2008
Received in revised form
6 March 2009
Accepted 11 May 2009
Available online 27 May 2009

Keywords:
Nonlinear acoustic diagnostics
Crack detection
Wave modulation spectroscopy

ABSTRACT

Despite the increasing number of impressive demonstrations of the high sensitivity of nonlinear-acoustic methods of damage detection, the physical factors which limit the ultimate sensitivity of this approach are not yet clearly understood. In this paper we perform the corresponding analysis and formulate criteria determining the minimal size of detectable cracks. The relation of the nonlinear-modulation technique to the linear frequency-shift technique is discussed. The analysis is particularly focused on the nonlinear-modulation resonance technique. It is based on rather general properties of the defects consistently predicted by various rigorous cracks models. The obtained conclusions are compared with experimental data obtained in nonlinear-modulation experiments on the detection of cracks in railway axles and wheels.

1. Introduction

The nonlinear-acoustic technique for early crack detection is actively studied in recent years (see, for example, [1–13]). High sensitivity of this approach is considered as one of the most attractive features of this methodology and is directly related to its physical principle. Indeed, it is well known that for homogeneous solids, their elastic nonlinearity is mostly determined by the weak anharmonicity of the interatomic potential [15]. In the simplest case of longitudinal deformation, such nonlinearity can be characterized by dimensionless coefficients in the power-series expansion of the material stress–strain relationship, $\sigma = E[\varepsilon + \beta\varepsilon^2 + \cdots]$, where σ is the stress, ε the strain, E the elastic modulus, and β the quadratic nonlinearity parameter. Its typical value is on the order of several units [15], which means that for typical acoustic strains $\varepsilon < 10^{-5}$, the relative level of the lowest-order nonlinear correction $\sim\beta\varepsilon$ due to the quadratic term is very small (-85 to -95 dB). Therefore, usually the quadratic approximation is sufficient in most practical cases and higher-order nonlinear terms are not taken into account.

The presence of such defects as cracks often strongly increases the sample effective nonlinearity. Indeed, at crack's perimeter and at inner contacts, the strain and stress are locally strongly (orders of magnitude) enhanced, so that the strongest deviation from the linear Hooke's law is localized at these "weak" defects. If the defect size and/or concentration are not too small, then the average sample nonlinearity strongly increases thus indicating the presence of damage. To detect this defect-induced growth of the sample nonlinearity, the nonlinear-modulation technique is considered to be one of the most sensitive methods [5]. It is usually used in the resonance variant [1,2,8,13,14,16] in which a relatively high-frequency (probe) wave is excited in the sample together with a lower-frequency wave (pump) and the level of the resultant probe-wave modulation is observed.

Independent impressive demonstrations of the superior sensitivity of the nonlinear-acoustic approach compared to linear methods are known [1–14,16]. The main concern in the feasibility of this approach is related to ensuring sufficiently high linearity of the transducers (including their proper coupling), of the supporting systems and electronic equipment, whereas the background atomic nonlinearity of the intact material is usually considered as a negligible factor (see, for example, [5]). The sufficient linearity of the entire measurement system is conventionally verified by comparing the observed levels of nonlinear distortions in damaged and reference intact samples. However, the role of the background atomic nonlinearity in intact samples and the ultimate sensitivity of the nonlinear acoustic methods (i.e., the criteria of the minimal detectable crack size) are not yet clearly understood. The present study is intended to fill this gap and to provide better insight in the physical factors determining the ultimate sensitivity of the nonlinear-acoustic technique for damage detection.

2. The role of the background atomic nonlinearity

Let us first estimate the background level on the combinational-frequency components arising due to the distributed

* Corresponding author. Tel.: +78314164872; fax: +78314365976.
E-mail address: vyuzai@mail.ru (V.Yu. Zaitsev).

0963-8695/$ - see front matter © 2009 Elsevier Ltd. All rights reserved.
doi:10.1016/j.ndteint.2009.05.001

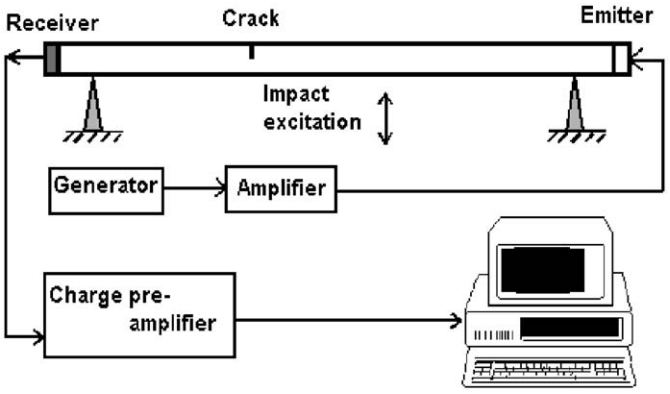

Fig. 1. Schematically shown configuration of nonlinear-modulation experiments [16].

atomic nonlinearity of solids. For further comparison with observation data, we will use experiments [16] on the nonlinear-modulation detection of cracks in railway axles and disks in real industrial conditions of a railway workshop. Since the original Ref. [16] is not easily accessible, Fig. 1 schematically shows the experimental configuration. Both intact and crack-containing samples were studied. In some cases the cracks were natural and in the other for calibration and testing, we used artificial crack-like defects in the form of saw-cuts of about 1–2 mm width and 5–8 mm in depth with tightly inserted metal plates to imitate contacting crack interfaces.

As a reasonable model of an axle we choose a rod-shape resonator. However, the instructive 1D approximation is not critical for the main conclusions. Here, we also limit ourselves to the discussion of longitudinal acoustic excitations (the Young modes), which suffice to analyze the main factors determining the ultimate (threshold) sensitivity of the nonlinear-modulation method. We thus start from the 1D wave equation

$$\rho\partial^2 u/\partial t^2 = \partial\sigma/\partial x, \tag{1}$$

where ρ is the material density, u the particle displacement from the equilibrium position, and σ the stress. We assume that the material can be described by a nearly Hookean law

$$\sigma = E[\partial u/\partial x + F(\partial u/\partial x)] + g\partial^2 u/\partial x\partial t, \tag{2}$$

where E is the elastic modulus and the terms $F(\partial u/\partial x)$ and $g\partial^2 u/\partial x\partial t$ are responsible for the weak (i.e., $F(\partial u/\partial x) \ll \partial u/\partial x$) atomic nonlinearity of the material and linear viscous-like losses, respectively. Eqs. (2) and (1) yield the following wave equation:

$$\frac{\partial^2 u}{\partial t^2} - c_0^2\frac{\partial^2 u}{\partial x^2} - c_0^2\frac{\partial}{\partial x}F\left(\frac{\partial u}{\partial x}\right) - \frac{g}{\rho}\frac{\partial^3 u}{\partial t\partial x^2} = 0, \tag{3}$$

where $c_0 = (E/\rho)^{1/2}$ is the acoustic-wave velocity. Various aspects of nonlinear transformations of acoustic excitations in resonators have been widely discussed in literature (higher harmonic generation, parametric instabilities, nonlinear resonances, etc., see, for example, books [17,18]). However, to get the explicit expressions for modulational components produced by interactic eigenmodes, we briefly recall the conventional perturbation procedure for a rod-like sample of length L with the following characteristic boundary conditions:

$$u(x=0) = u(x=L) = 0 \quad \text{(two rigid boundaries)} \tag{4a}$$

$$u(x=0) = 0, \quad \partial u/\partial x(x=L) = 0 \quad \text{(one rigid and free boundary)} \tag{4b}$$

$$\partial u/\partial x(x=0) = 0, \quad \partial u/\partial x(x=L) = 0 \quad \text{(two free boundaries)} \tag{4c}$$

For boundary conditions (4a)–(4c), we expand the displacement field in the resonator into series in the eigenfunctions ψ_n (sinusoidal in the discussed case):

$$u(x) = \sum_i A_i(t)\sin(k_i x), \quad k_i = (\pi/L)i, \tag{5a}$$

$$u(x) = \sum_i A_i(t)\sin(k_i x), \quad k_i = (\pi/2L)(2i-1), \tag{5b}$$

$$u(x) = \sum_i A_i(t)\cos(k_i x), \quad k_i = (\pi/L)i, \tag{5c}$$

In Eqs. (5a)–(5c), the eigenfunctions are non-normalized, so that factors A_i directly correspond to the displacement amplitude in each eigenmode.

Retaining in the nonlinear function $F(u_x)$ only the lowest quadratic term with the nonlinear parameter β,

$$F(\partial u/\partial x) = \beta(\partial u/\partial x)^2, \tag{6}$$

and taking into account orthogonality of the eigenfunctions we obtain from Eqs. (3), (5) and (6) the following equations for the displacement amplitude A_n of nth eigenmode which interacts with other modes due to the quadratic nonlinearity:

$$\ddot{A}_n + 2\nu_n\dot{A}_n + c_0^2 k_n^2 A_n = \beta\frac{c_0^2}{L}\sum_{mp} k_m k_p A_m A_p a_{mp}^n. \tag{7}$$

Taking into account that $k_n A_n = S_n$ is the strain amplitude for the nth mode, we rewrite Eq. (7) as

$$\ddot{S}_n + 2\nu_n\dot{S}_n + \omega_n^2 S_n = \beta\omega_n^2\sum_{mp} S_m S_p \tilde{a}_{mp}^n. \tag{8}$$

The interaction coefficients $\tilde{a}_{mp}^n$ will be specified below; $\omega_n = c_0 k_n$ is the nth mode eigenfrequency, and $\nu_n = gk_n^2/(2\rho)$ is the dissipation coefficient (in what follows, it will be more convenient to pass to Q-factors $Q_n = \omega_n/(2\nu_n)$ of the corresponding modes, which can readily be estimated from experimental data).

For modes with the eigenfunctions ψ_m, ψ_p, and ψ_n, the interaction coefficients are related to the mode structures via integrals of the form,

$$\int_0^L \psi^{(n)}\psi_x^{(m)}\psi_{xx}^{(p)}\,dx$$

which yield the following coefficients $\tilde{a}_{mp}^n$ (for boundary conditions (4a)–(4c), respectively):

$$\tilde{a}_{mp}^n = \frac{\delta_{n,p\pm m}}{2} \quad \text{(where } \delta_{n,p\pm m} \text{ is the Kronecker delta)}, \tag{9a}$$

$$\tilde{a}_{mp}^n = \frac{8(2m+1)(2p+1)(2n+1)(-1)^{m+n+p+1}}{\pi[(2n-1-2m-2p)(2n+1+2m-2p)(2n-1-2m+2p)(2n+3+2m+2p)]}, \tag{9b}$$

$$\tilde{a}_{mp}^n = \frac{4mpn[-1+(-1)^{m+p+n}]}{\pi[(m+p)^2-n^2][(p-m)^2-n^2]}. \tag{9c}$$

To estimate the amplitudes of the modulation sidelobe corresponding to nth mode we assume that initially the probe mode S_p with strain amplitude $S_p^{(0)}$ and frequency $\omega_p^{(0)}$ is excited in the sample together with a low-frequency pump mode S_m with amplitude $S_m^{(0)}$ and frequency $\omega_m^{(0)}$:

$$S_p = S_p^{(0)}[\exp(i\omega_p^{(0)}t) + \exp(-i\omega_p^{(0)}t)]/2, \tag{10}$$

$$S_m = S_m^{(0)}[\exp(i\omega_m^{(0)}t) + \exp(-i\omega_m^{(0)}t)]/2. \quad (11)$$

Note that frequencies $\omega_p^{(0)}$ and $\omega_m^{(0)}$ do not necessarily coincide with eigenfrequencies ω_p and ω_m of the closest pth and mth modes. According to Eq. (8), these modes create for mode number n (i.e., the modulation sidelobe), nonlinear sources $\propto S_m S_p$ at frequencies $\omega_p^{(0)} \pm \omega_m^{(0)}$. To estimate the maximum level of the modulation, we assume that the combination frequency coincides with the eigenfrequency ω_n of the nth mode, $\omega_n = \omega_p^{(0)} \pm \omega_m^{(0)}$. Then Eq. (8) yields for the relative level of the resultant modulation:

$$\frac{S_n^{(0)}}{S_p^{(0)}} = S_m^{(0)} \frac{\omega_n}{4v_n} \beta \tilde{a}_{mp}^n = S_m^{(0)} Q_n \frac{1}{2} \beta \tilde{a}_{mp}^n. \quad (12)$$

Besides quite evident dependence on the pump strain amplitude $S_m^{(0)}$, Q-factor Q_n of the combination-frequency mode, and nonlinearity coefficient β, the interaction essentially depends on the mode spatial structures via the interaction coefficient $\tilde{a}_{mp}^n$. If the frequencies of all three interacting modes coincide with the sample eigenfrequencies ($\omega_n = \omega_p \pm \omega_m$), then for a resonator with two rigid boundaries (at which the reflected waves do not experience phase jumps), the spatial-resonance condition $k_p \pm k_m = k_n$ (equivalent to $p \pm m = n$) is also satisfied and corresponds to the coefficient $\tilde{a}_{mp}^n = 0.5$. Assuming the typical Q-factor value $Q_p \sim 500 \ldots 1000$ for the probe-mode with numbers $p \sim 50 \ldots 60$ and pump-strain amplitude $S_m^{(0)}$ in the range $(0.5–1) \times 10^{-5}$ as in experiments [16] and taking the nonlinearity parameter value $\beta = 3 \ldots 6$ (which is typical for homogeneous solids [15]), we obtain the modulation-level estimate

$$S_n/S_p^{(0)} \sim -(35 \ldots 45)\text{dB}. \quad (13)$$

These values significantly exceed the simplest quasistatic estimate discussed in the introduction which corresponds to $S_n/S_p^{(0)} \sim -(85 \ldots 95)$dB for the same assumptions as in estimate (13).

For samples with non-rigid boundaries, which produce mutual phase shifts for interacting waves, the spatial and frequency resonance conditions usually cannot be satisfied simultaneously (except of very particular mode combinations m, p and n in the case of a non-equidistant mode spectrum). Acoustically soft (free) boundaries (Eq. (4c)) produce especially strong phase mismatch resulting in zero interaction coefficient $\tilde{a}_{mp}^n = 0$ when the interacting-wave frequencies exactly coincide with the eigenfrequencies (i.e., $\omega_n = \omega_p \pm \omega_m$). However, this does not mean that the modulation interaction is completely forbidden for such samples, since quite non-negligible non-resonant interaction remains possible. Consider, for example, the conditions of experiments [16] in which the impact-excited pump corresponded to low-numbers modes (e.g., $m = 1 \ldots 5$) in the frequency range of several kHz and the ultrasonic probe wave in the range 50–70 kHz corresponded to longitudinal-mode numbers $p = 50 \ldots 70$ in resonating railway axles. Then for two free ends of the resonator, Eq. (9c) indicates that for the pump-mode number $m = 2$, the probe-mode number $P = 60$, and the combinational-component numbers $n = 60 \pm 2$ (which satisfy the frequency condition $\omega_n = \omega_p \pm \omega_m$), the interaction is impossible since $\tilde{a}_{mp}^n = 0$. Nevertheless, for the same frequencies ω_p, ω_m, and ω_n, the sidelobe mode $n = 62$ can be excited due to non-resonant interaction of the pump mode $m = 2$ and the probe mode $P = 61 \neq 60+2$, for which $\tilde{a}_{mp}^n = 0.42$ (i.e., comparable with $\tilde{a}_{mp}^n = 0.5$ for the rigid boundary conditions). Certainly, for the mode triplet $m = 2$, $n = 62$, and $P = 61$ the interaction is not optimal since for the frequency condition $\omega_p = \omega_n \pm \omega_m$, the mode $P = 61$ participating in the interaction is excited out of resonance. But for the considered sufficiently high mode numbers $P \gg 1$, the relative intermode distance is small, $\Delta\omega_p \sim \omega_p/p \ll \omega_p$ and even non-resonant neighboring modes can be excited fairly efficiently. For example, under the same assumptions as in the estimate (13) (the probe-wave frequencies $\sim 50 \ldots 70$ kHz and numbers $p \sim 50 \ldots 70$ and Q-factors about 500), the difference between the levels of resonant and neighboring non-resonant modes is only $\sim$20–25 dB. Correspondingly, compared to the resonant estimate (13) for the sample with rigid boundaries, the visible modulation depth should also be $\sim$20–25 dB lower,

$$S_n/S_p^{(0)} \sim -(55 \ldots 70)\,\text{dB} \quad (14)$$

which still strongly exceeds the simplest quasistatic estimate $S_n/S_p^{(0)} \sim \beta S_m^{(0)} \sim -(85 \ldots 95)$dB. It should be emphasized that eventual additional influence of the dispersion (which can be non-negligible for higher-number modes) does not change the estimated range of the modulation depth. Indeed, for the rigid boundaries, the additional dispersion-induced phase shift between the modes can decrease the resonant estimate (13) shifting it closer to the out-of-resonance value (14), but for the phase-inverting soft boundaries, this additional shift can on the contrary improve the interaction conditions and shift the out-of-resonance estimate (14) closer to the resonance case (13).

Note that in experiments, the interacting-wave frequencies normally are varied in a sufficiently wide range to reduce the uncertainty in the modulation level due to unknown exact resonance and dispersion conditions. A typical averaged example of such a modulation spectrum obtained in [16] for a reference intact axle is shown in Fig. 2. The figure demonstrates that quite conventional equipment used in [16] is sufficient to reliably observe the modulation level comparable with estimate (14) and even lower (since the probe wave level exceeds the background noise by 80–100 dB). Preliminary tests indicated that the nonlinearity of the electronics did not produce such well visible combinational components whose origin can reasonably be attributed to the atomic nonlinearity of the reference sample. Unlike technical noises further improvement of the equipment cannot eliminate this background modulation in principle.

The obtained estimates and the experimentally observed background modulation consistently indicate that the atomic nonlinearity is not negligible and determines the threshold level of the hindering signal, which imposes the physical limitation on the ultimate sensitivity of the nonlinear-acoustic approach. In what follows, we compare this estimate with the modulation-sidelobe level due to the presence of a crack-like defect in the

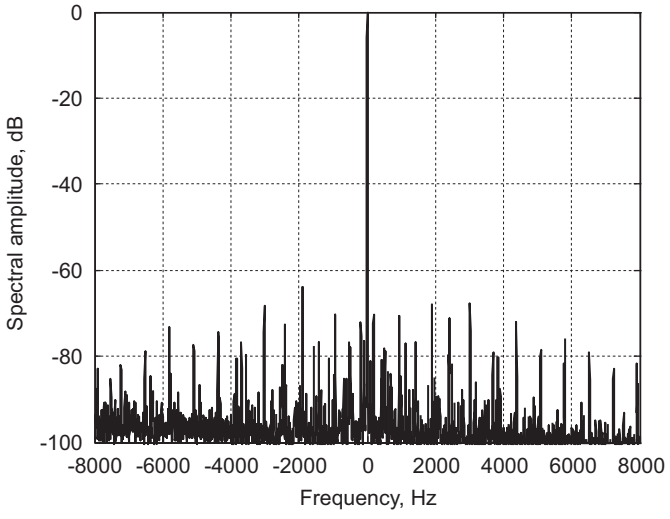

Fig. 2. Averaged modulation spectrum (centered to zero frequency) for an intact axle in experiments [16].

sample in order to formulate the criteria of the threshold (ultimate) sensitivity on the nonlinear-modulation approach.

3. Quasilinear and quasistatic estimation of the influence of crack-like defects

In this section, using a perturbation approach we first consider the influence of a crack-like defect on the sample eigenfrequencies (which is in fact a linear effect). Then we estimate the level of crack-induced modulation of a probe wave arising due to modulation of the crack-opening (and, consequently, eigenfrequency modulation) by an additional acoustic excitation. This will allow us to instructively compare the conventional linear frequency-shift technique [19] of crack detection and the nonlinear approach.

To obtain the wave equation with allowance for the crack presence, we use the Lagrangian approach. The sample is again supposed to have a rod-shape geometry with the cross-section area B_0. In order to comprise the defect into the Lagrangian density we use an instructive crack model which was earlier successfully used in [20–22] to describe elastic properties of 3D materials containing an ensemble of crack-like defects. In this approach, cracks are considered as equivalent planar soft inclusions characterized by the area B and thickness $h \ll B^{1/2}$. The inhomogeneity of the near-crack fields in this approach is not considered and the crack contribution is accounted as an addition to the elastic-energy density under conventional assumption that crack's size is much smaller than the characteristic scale of the variation in the average strain u_x in the material (in most cases this is the elastic wave length). In the 3D analysis [20–22], such defects were characterized by two effective elastic parameters corresponding to the crack compliance with respect to the external shear and normal (compressing) elastic stresses. For our purpose to obtain the upper estimates of the crack influence, it is sufficient to assume that the crack plane is oriented normally to the sample axis such that the defect can be characterized by one parameter of its normal compliance. Looking at the defect from aside (i.e., from a distance several times exceeding its diameter) it can be viewed as a planar "soft inclusion" characterized by the effective elastic modulus $\varsigma E \ll E$, where E is the elastic modulus of the surrounding homogeneous matrix material and $\varsigma \ll 1$ is the small parameter characterizing the increased compliance of the defect.

Various particular rigorously derived crack models consistently indicate that the above-introduced ς is approximately equal to the ratio of the crack opening h to its diameter D (i.e., its aspect ratio, $\varsigma \sim h/D$): such a crack can completely be closed by creating in the material the average strain S^* approximately equal to its aspect ratio $S^* \sim \varsigma \sim h/D \sim h/B^{1/2}$, where B is the crack cross-section [23]. Thus the (normal) compliance parameter ς accounts for the local enhancement in the "local strain": $\Delta h/h \sim u_x/\varsigma$, where the variation Δh in the crack opening is caused by the ambient stress $\sigma = E\partial u/\partial x$. Then for the crack orthogonal to the sample axis, the elastic-energy density W_{def} related to the presence for the defect can be written as

$$W = \delta(x - x_0)(Bh)E\frac{(\partial u/\partial x)^2}{(2\varsigma)} = \delta(x - x_0)B^{3/2}\frac{(\partial u/\partial x)^2}{2}, \tag{15}$$

where $\delta(..)$ is the Dirac delta-function, x_0 is the coordinate of the defect. The normalization factor before the delta function is the well-known total elastic energy localized near the crack, which is proportional to the volume of the sphere circumscribed around the crack (i.e., the effective crack volume $\tilde{V} \sim B^{3/2}$). Such an energy approach developed in [20–22] leads to results consistent with other models of elastic properties of crack-containing solids based on particular crack models (e.g.,[23,24]) and gives additional freedom in modeling the material elastic and dissipative properties for arbitrary ratios of the normal and shear compliance parameters of the defects.

Combining Eq. (15) for the energy localized at the crack with the conventional expression [26] for the density of the Lagrangian in the homogeneous solid, we obtain the Lagrangian density per unit length for the considered rod-shape sample containing a crack-like defect at $x = x_0$:

$$L = (1/2)\left\{(\partial u/\partial t)^2 - E(\partial u/\partial x)^2\right\}B_0 - \delta(x - x_0)\tilde{V}\frac{(\partial u/\partial x)^2}{2}. \tag{16}$$

Here, we yet neglect the nonlinearity of the crack and also omit the distributed nonlinearity which has already been considered in the previous section. By the conventional procedure [26] we obtain form Eq. (16) the following wave equation:

$$\frac{\partial^2 u}{\partial t^2} - c_0^2\frac{\partial^2 u}{\partial x^2} - c_0^2\frac{\partial}{\partial x}\left\{\delta(x - x_0)\frac{\tilde{V}}{B_0}\frac{\partial u}{\partial x}\right\} = 0. \tag{17}$$

The boundary conditions for Eq. (17) are given by Eqs. (4a)–(4c). Eq. (17) indicates that in the linear approximation, the effect of the crack presence is determined by its effective volume $\tilde{V}$ and is practically independent on specific features of a particular crack model.

Using Eq. (17) we can readily estimate the eigenfrequency shifts due to the presence of the crack-like defect. As above representing the displacement field as the superposition of the sample eigenmodes $u = \sum_n A_n\psi^{(n)}(x)$ and substituting of this expansion in Eq. (17) we obtain the system of equations for the amplitudes A_n of the eigenmodes

$$\sum_n\left\{\ddot{A}_n\psi^{(n)}(x) - c_0^2\psi_{xx}^{(n)}A_n - c_0^2\frac{\partial}{\partial x}\left[\delta(x - x_0)\frac{\tilde{V}}{B_0}\psi_x^{(n)}\right]A_n\right\} = 0, \tag{18}$$

where the subscript at $\psi_x^{(n)}$ denotes differentiation d/dx. To estimate the crack-produced variations of the eigenfrequencies we apply to Eq. (18) the perturbation approach (similar to that used in quantum mechanics to estimate energy-level perturbations [27]). In the zeroth order (i.e., in the absence of the defect), the variables in Eq. (18) can be separated. The unperturbed eigenfunctions $\psi^{(n)}$ satisfy the equation

$$\frac{\ddot{A}_n}{A_n} = \frac{c_0^2\psi_{xx}^{(n)}}{\psi^{(n)}} = -k_n^2c_0^2. \tag{19}$$

The eigenvalues for the wavenumber k_n^2 (and the equivalent eigenfrequencies $\omega_n^2 = c_0^2k_n^2$) are determined by boundary conditions (4a)–(4c) next order of the perturbation theory [27], one can assume that the eigenfunction forms are approximately unperturbed and the perturbation (the presence of the defect) is reduced to the perturbation of the eigenvalues: $\omega_n^2 \to \omega_n^2 + \delta(\omega_n^2)$. Substituting the perturbed eigenvalues in Eq. (18) and taking into account Eq. (19) we obtain

$$\sum_n\left\{\delta(\omega_n^2)\psi^{(n)}(x) + c_0^2\frac{\partial}{\partial x}\left[\delta(x - x_0)\frac{\tilde{V}}{B_0}\psi_x^{(n)}\right]\right\} = 0. \tag{20}$$

Using the orthogonality of the eigenfunctions $\psi^{(n)}$ we find the required expression for the eigenfrequency perturbation:

$$\frac{\delta(\omega_n^2)}{\omega_n^2} = \frac{c_0^2}{\omega_n^2}[\psi_x^{(n)}(x_0)]^2\frac{2\tilde{V}}{S_0L} = \frac{1}{k_n^2}[\psi_x^{(n)}(x_0)]^2\frac{2\tilde{V}}{V_0}, \tag{21}$$

where $V_0 = B_0L$ is the sample volume, $\psi_x^{(n)}$ is the derivative of the eigenfunction for the particle displacements with respect to x (so $\psi_x^{(n)}$ is the eigenfunction for strain) and combination $\psi_x^{(n)}/k_n$ corresponds to the displacement eigenfunctions $\psi^{(n)}$ with

maximum values equal to unity. Eq. (21) shows that the relative variation in the nth mode eigenfrequency is entirely determined by the crack position x_0 and the ratio of the effective volume $\tilde{V}$ of the defect to the volume V_0 of the sample. In the strain nodes ($\psi_x^{(n)}(x_0)=0$), the crack does not affect the corresponding eigenfrequency and in the antinodes (where $[\psi_x^{(n)}(x_0)/k_n]^2=1$), the crack effect is maximum, such that

$$\delta\omega_n/\omega_n \le \tilde{V}/V_0. \tag{22}$$

If this eigenfrequency shift exceeds certain threshold value $(\delta\omega_n/\omega_n)_{th}$, the conclusion on the presence a crack can be made [19]. Therefore, the minimal size of the detectable crack (in terms of the effective crack volume $\tilde{V}\sim D^3$) is determined by the threshold value $(\delta\omega_n/\omega_n)_{th}$, such that Eq. (22) can be rewritten as

$$\tilde{V} \ge (\delta\omega_n/\omega_n)_{th} V_0. \tag{23}$$

Typically it is assumed that meaningful variations in the sample frequency should be on the order of at least 2…5% [19], because smaller variations can be caused by many other factors (e.g., temperature variations) not related to the damage. Since the sample volume is proportional to the third power of its characteristic linear dimension, it follows from Eq. (23) that this meaningful threshold variation $(\delta\omega_n/\omega_n)_{th}\sim(2\ldots5)\times10^{-2}$ is only reached if the crack size reaches 20–40% of the entire sample size (and for elongated rod-shape samples, the detectable crack size can even reach 50–60% of the sample diameter). Such a large size of detectable defects is normally unacceptable from the viewpoint of security, but significant reduction in the threshold $(\delta\omega_n/\omega_n)_{th}$ is not possible in view of strong increase of false alarms. Therefore, other ways of improving the detection sensitivity are of evident interest, in particular, the nonlinear-modulation techniques.

From this point of view, relationship (23) readily allows one to estimate of the detectable defect size in the nonlinear-modulation methodology. To this end, we recall that the effective volume $\tilde{V}$ of the defect can be modulated by an additional acoustic action (pump). As it was already mentioned, the average strain $u_x^* \equiv S^*\sim h/D$ in the material is able to completely close the crack with opening h and characteristic size D. Therefore, the dependence of the effective volume variation $\Delta\tilde{V}$ on the average strain in the sample can be approximated by the following evident expression:

$$\Delta\tilde{V} \approx (S/S^*)\tilde{V}. \tag{24}$$

According to Eq. (21), this variation in the effective crack volume should produce corresponding variations in the eigenfrequencies ω_n. In turn, the variation in the sample eigenfrequency causes the amplitude-phase modulation of a probe wave excited in the vicinity of this sample resonance. The resultant modulation depth for the probe wave can be especially simply estimated in the approximation of sufficiently slow modulation. We first assume that the characteristic modulation period T_m is larger than the characteristic transient time of resonant excitation of the considered eigenmode (i.e., $T_m > Q_n/\omega_n$, where Q_n is the mode Q-factor). This means that the current amplitude of the probe wave is determined by the current value of the nearest resonance frequency.

Near the eigenmode number p, the probe-wave amplitude is described by an equation with the left-hand side coinciding with that of Eqs. (7) and (8) and with an external probe-wave source $F_{ext}(t)$ in the right-hand side:

$$\ddot{S}_p + 2v_p\dot{S}_p + \omega_p^2 S_p = F_{ext}(t). \tag{25}$$

For a sinusoidal source $F_{ext}(t)=F_0\exp(i\omega t)$, the resultant amplitude A_p is given by the expression

$$S_p = \frac{F_0}{(\omega_p^2-\omega^2)+2iv_p\omega}. \tag{26}$$

Correspondingly, the mode intensity is

$$I_p \equiv |S_p|^2 = \frac{|F_p|^2}{(\omega_p^2-\omega^2)^2+4\omega^2\omega_p^2/Q_p^2}. \tag{27}$$

For sufficiently small detuning $|\omega_p-\omega|\ll\omega_p$ and sufficiently high Q-factor $Q_p\gg1$, Eq. (27) for the normalized intensity $\tilde{I}=I/I_{\max}$ can be approximated by a Lorentzian curve

$$\tilde{I}_n = \frac{1}{[2Q_n(\omega_n-\omega)/\omega_n]^2+1} = \frac{1}{(2Q_n\Delta)^2+1}, \tag{28}$$

where $\Delta=(\omega_n-\omega)/\omega_n$ is the dimensionless detuning. For this function, the maximum derivative $d\tilde{I}_n/d\Delta = 3\sqrt{3}Q_p/4 \approx Q_p$ is reached for the initial detuning $\Delta = 2\Delta Q_p = 1/\sqrt{3}$ (i.e., at the resonance slope). Therefore, for a probe wave excited at the resonance-curve slope, the additional acoustic-pump action $S_m^{(0)}$ should produce the variable detuning $\Delta=\Delta(S_m^{(0)})$ which, according to Eqs. (26)–(28), produces the variation in the probe-wave amplitude

$$|\Delta S_p/S_p| \approx Q_p\Delta(S_m^{(0)}). \tag{29}$$

By virtue of Eqs. (21) and (24) we then obtain that the modulation of the probe-wave amplitude is related to the pump amplitude $S_m^{(0)}$ by

$$\frac{\Delta S_p}{S_p} \approx Q_p\frac{S_m^{(0)}}{S^*}\frac{\tilde{V}}{V_0}\frac{1}{k_n^2}[\psi_x^{(n)}(x_0)]^2 \le Q_p\frac{S_m^{(0)}}{S^*}\frac{\tilde{V}}{V_0}. \tag{30}$$

Now we have to compare this crack-induced modulation level $\Delta S_p/S_p$ given by Eq. (30) with the relative sidelobe amplitude S_n/S_p given by Eq. (12) for the background (hindering) modulation produced by the distributed atomic nonlinearity of the sample. Since for sufficiently high-number modes the Q-factors are comparable, $Q_n\approx Q_p$, comparison of Eqs. (30) and (12) gives us the required criterion of the threshold effective volume $\tilde{V}$ of detectable cracks:

$$\frac{\tilde{V}}{S^*V_0}\sim\beta\tilde{a}_{mp}^n/2. \tag{31}$$

Note that the parameter combination $\beta\tilde{a}_{mp}^n/2$ in the right-hand side of Eq. (31) is on the order of unity for the most part of materials, such that the threshold effective volume of the crack can be written as

$$\tilde{V} \ge V_0 S^* \tag{32}$$

The structure of Eq. (32) is similar to that of estimate (23) obtained for the conventional frequency-shift technique [19]. However, in contrast to Eq. (23), in which the threshold frequency variation $(\delta\omega_n/\omega_n)_{th}$ is on the order of $(2\ldots5)\times10^{-2}$ [19], in Eq. (32), the same role is played by the much smaller factor S^* which is closely related to the softness of the crack and is approximately equal to the crack aspect ratio, $S^*\sim h/D$. We underscore that estimate (32) is fairly universal and does not depend on details of a particular crack model. Eq. (32) clearly indicates that in the nonlinear-modulation approach, not only the crack size, but also the crack softness (and, consequently, its aspect ratio) plays the key role. It is known that for thin cracks, the aspect ratio and thus the factor S^* in Eq. (32) can be as small as $S^*\sim10^{-5}$ and even less. Thus, the comparison of Eqs. (23) and (32) containing the factors $(\delta\omega_n/\omega_n)_{th}\sim(1\ldots2)\times10^{-2}$ and $S^*\sim10^{-5}$, respectively, demonstrates the superior sensitivity of the nonlinear-modulation approach, especially for detection of just appearing thin cracks.

As an instructive example, let us consider a typical railway axle with length ~2 m and radius varying within 7–9 cm corresponding to the sample volume $V_0\approx0.04\,\mathrm{m}^3$. Therefore, for thin cracks with $S^*\sim10^{-5}\ldots10^{-6}$, Eq. (32) yields the threshold value of the

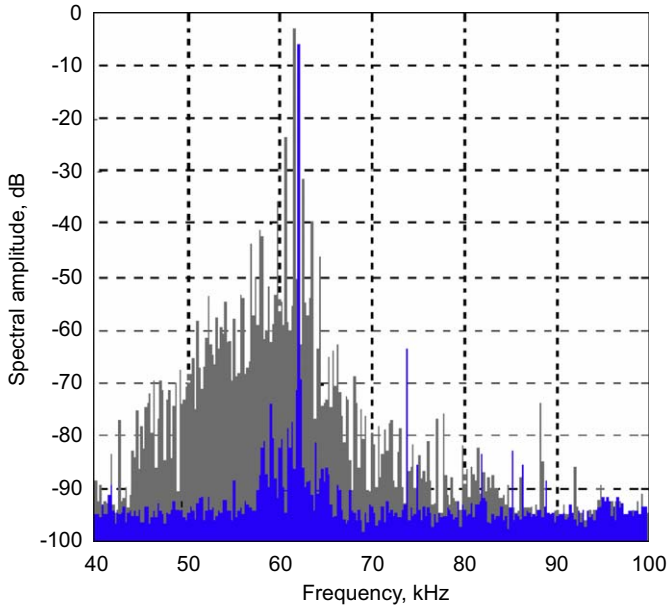

Fig. 3. An example of superimposed modulation spectra obtained in experiments [16] for an intact axle (dark color) and an axle with a thin transversal crack with ~1 cm size. (For interpretation of the references to the color in this figure legend, the reader is referred to the web version of this article.)

effective crack volume $\tilde{V}\sim 4\times(10^{-7}\ldots 10^{-8})\,\mathrm{m}^3$, which ensures the probe-wave modulation depth comparable with the background modulation due to the atomic nonlinearity of the material. This estimate corresponds to the characteristic crack size $D\sim\tilde{V}^{1/3}\sim 3\ldots 7\,\mathrm{mm}$. This means that a somewhat larger single thin crack with the size $D\sim$10–15 mm can produce the modulation of the probe wave at a level of $-(40\ldots 30)\,\mathrm{dB}$ which should 20–40 dB exceed the background level due to the atomic nonlinearity estimated in the previous section. These estimates well agree with the data obtained in experiments [16]. An example of the modulation spectrum in an axle containing such a single fatigue-induced crack is shown in Fig. 3 together with a spectrum obtained for an intact axle in similar conditions.

4. Dynamic estimation of the modulation-level for a nonlinear crack model

The instructive estimate of the crack-induced modulation in the previous section is found in the quasistatic case where the modulation is so slow that the probe-wave amplitude excited close to a resonance is determined by the current resonance position. Now we estimate the level of a non-quasistatic modulation by combining the approaches used in two previous sections.

Let us now retain the leading nonlinear term in the expression describing the crack response to the applied stress (bearing in mind that the main nonlinear correction is quadratic). Certainly, for pump strains strongly exceeding the above introduced characteristic strain $S^*\sim h/D$, the crack should exhibit near-complete closing and opening. Consequently, its nonlinearity should become non-analytic (clapping/piecewise like discussed in [6,7,13]) rather than quadratic. Additionally, adhesion and/or frictional phenomena at the crack interfaces can result in hysteretic effects [9]. However, bearing in mind that typically $S^*\sim h/D$ is on the order of $10^{-3}\ldots 10^{-5}$, for moderately intensive pump strains (e.g., $S^{(0)}\leq 10^{-6}\ldots 10^{-5}$) often applied in practice, one can use a quadratic approximation for the crack nonlinearity (like in [8]). Experimentally, this is justified by the fact that quite often the modulation sidelobes are near-linearly proportional to the pump-wave amplitude in a fairly wide strain range, which indicates a quadratic character of the nonlinearity (see, for example, [7,8,14,16]) and only for stronger pump amplitudes, the modulation level increases slower and often tends to saturation [7,8]. Therefore, for moderate amplitudes, the quadratic approximation is reasonable, so that the average stress σ in the material can be related to the local strain $S_{loc}=\Delta h/h$ characterizing the variation in the crack opening h as

$$\sigma = S_{loc}E_{eff}(1+\beta_c S_{loc}), \tag{33}$$

where E_{eff} is the effective crack modulus (which is strongly reduced compared to the elastic modulus of the intact material, $E_{eff}\sim\varsigma E$) and β_c the local parameter of the crack nonlinearity. To estimate its value one can argue that in the first approximation (neglecting the nonlinearity), the local strain S_{loc} and the mean strain S are related via the parameter ς of the crack softness, $S_{loc}=S/\varsigma$. On the other hand, we note that for the characteristic strain $S^*\sim\varsigma$ causing the crack closure, the variation in the crack opening is equal to its initial opening ($S_{loc}\sim 1$) and the completely closed crack is not soft anymore (i.e., the variation in its elastic modulus is comparable with its initial value). This means that the nonlinear term $\beta_c S_{loc}$ in the braces in Eq. (33) is comparable with unity ($\beta_c S_{loc}\sim 1$) for $S_{loc}\sim 1$. Therefore, the local nonlinearity parameter is also on the order of unity, $\beta_c\sim 1$, which will be used in the estimates below. Note that the considered approximation is also consistent with Eq. (24) in the previous section, where we also took into account that with increasing average strain the effective volume of the crack gradually decreases and for compressing strains $S\sim S^*\sim\varsigma$, the crack is almost completely closed.

The quadratic stress–strain relationship (33) corresponds to retaining the cubic term in the expression for the crack energy, so that instead of Eq. (15) we have

$$W=\delta(x-x_0)(Bh)E\left\{\frac{(\partial u/\partial x)^2}{2\varsigma}+\beta_c\frac{(\partial u/\partial x)^3}{3\varsigma^2}\right\} \tag{34}$$

Combining this expression with the Lagrangian density for the homogenous matrix material (like in the derivation of Eq. (17)), we obtain the following wave equation (in which again the atomic nonlinearity is omitted):

$$\frac{\partial^2 u}{\partial t^2}-c_0^2\frac{\partial^2 u}{\partial x^2} - c_0^2\frac{\partial}{\partial x}\left\{\delta(x-x_0)\frac{Bh}{B_0\varsigma}\frac{\partial u}{\partial x}+\delta(x-x_0)\beta_c\frac{Bh}{B_0\varsigma^2}\left(\frac{\partial u}{\partial x}\right)^2\right\}=0. \tag{35}$$

Here, like for Eq. (18) we have to take into account that $\varsigma\sim h/B^{1/2}$ and $Bh/B_0\varsigma\sim\tilde{V}/B_0$, where $\tilde{V}\sim B^{3/2}$ and $\varsigma\sim S^*$. Since for different boundary conditions the results are very similar and differ only by the phase of the sinusoidal eigenfunctions, below we limit ourselves only to the case of free boundaries and perform a procedure similar to that used above in the estimation of the modulation due to the quadratic atomic nonlinearity. Using the same assumptions on the initially excited probe and pump modes, we come to the following equation for the combination-mode strain (which is analogous to Eq. (8)):

$$\ddot{S}_n+2\nu_n\dot{S}_n+\bar{\omega}_n^2 S_n=\beta_c\omega_n^2\frac{2\tilde{V}}{S^*V_0}\sum_{mp}S_mS_p\,\sin(k_mx_0)\sin(k_px_0). \tag{36}$$

Here, frequency $\bar{\omega}_n$ of the nth mode is corrected in the first approximation for the presence of the crack (as discussed in the previous section). Considering again the resonance excitation of the nth mode by the combination-frequency source created by the

interaction of the pump mode $S_m^{(0)}$ and the probe wave mode $S_p^{(0)}$, we obtain

$$\frac{S_n^{(0)}}{S_p^{(0)}} = Q_n \frac{S_m^{(0)}}{S^*}\frac{\tilde{V}}{V_0} 2\beta_c \sin(k_m x_0) \sin(k_p x_0) \sim Q_n \frac{S_m^{(0)}}{S^*}\frac{\tilde{V}}{V_0} \quad (37)$$

Here, we took into account that $\sin(k_m x_0)\sin(k_p x_0) \le 1$ and $\beta_c \sim 1$. Since $Q_n \sim Q_p$, it is clear that Eq. (37) agrees with the quasistatic Eq. (30) with an accuracy of a factor of two (i.e., within the accuracy of the initial assumptions) and all the numerical estimates remain valid.

5. Conclusions

In the performed analysis we used well-established crack properties consistently supported by different rigorous crack models; the main conclusions and estimates are rather robust with respect to fine details of the crack-nonlinearity models. The analysis revealed the following critical factors. One key factor is the maximal crack-produced variation in the sample eigenfrequencies (it is proportional to the effective crack volume $\tilde{V}$ and thus determines the ultimate sensitivity of conventional linear methods [19] based on crack-produced change in eigenfrequencies). In the nonlinear-modulation approach, there is an additional key factor, the crack sensitivity to the acoustic-pump action, which is conveniently characterized by strain S^* required to completely close a thin crack. The obtained results allowed us to quantify the statements (see e.g., [5]) about the extremely high sensitivity of the nonlinear-acoustic approach and to demonstrate the similarity and differences and to compare ultimate sensitivities of the nonlinear-modulation technique and linear frequency-shift approach. Certainly the actual sensitivity of both the linear and nonlinear methods will be reduced if the conditions of the crack interaction with sounding fields are unfavorable (i.e., the crack is located near stress nodes or its plane is parallel to the acoustic stress).

Although for clarity of the analysis we used a 1D model, allowance for more complex mode structures will affect only the values of the interaction coefficients for the distributed nonlinearity. These coefficients will be determined by 3D convolutions of the type $\int \psi_m(\vec{r})\psi_p(\vec{r})\,d\vec{r}$ and the equivalent combinations of the type $\psi_m(\vec{r}_0)\psi_p(\vec{r}_0)$ instead of $\sin(k_m x_0)\sin(k_p x_0)$ in Eqs. (30) and (37) for the localized defects' nonlinearity. These modifications evidently cannot significantly affect the estimated proportion between the contributions of the distributed and localized nonlinearities. The same note remains valid if instead of the modulation sidelobes we would compare the second harmonic levels (although in practice this technique is less robust in terms of the presence of parasite nonlinearities in the equipment and in the sample support).

The comparison with typical nonlinear-modulation experiments [16] has shown that the modulation level observed in intact reference samples is within the theoretically estimated range, which means that for presently available experimental equipment, the distributed atomic nonlinearity (rather than technical nonlinearities) can already become the main physical factor which limits the ultimate (threshold) sensitivity of the nonlinear-acoustic methodology of crack detection based on the observation of first-order combination components.

To further increase the ultimate sensitivity of the nonlinear-acoustic methods, instead of the considered conventional modulation or second-harmonic generation, one can use higher-order nonlinear effects, for which the background contribution of the atomic nonlinearity can be significantly lower. On the other hand, due to non-classical features of crack's nonlinearity, the intensity of such effects in samples with cracks can be comparable with lower-order nonlinear effects. For example, the cross-modulation and cascade modulation interactions (higher-order in conventional terms) can be proposed [28,29]. To describe such effects, certainly the quadratic approximation is insufficient and more fine features of crack's nonlinearity (e.g., its non-analyticity typical of hysteretic or clapping-contact nonlinearity) are essential. Since for higher-order interactions the level of hindering effects due the atomic nonlinearity should be drastically lower, the physical limit of the ultimate detection sensitivity can be strongly improved. However, for such an approach, instead of the atomic nonlinearity the main problem should become the reduction of hindering non-quadratic technical nonlinearities in the electronics, transducers (including their coupling to the sample) and sample-supporting systems. The same note relates to the reduction of ambient noises. Despite these difficulties, there are reasons (see e.g., [25,26]) to expect that this way can be promising for further increase in the sensitivity of the nonlinear-acoustic approach.

Acknowledgments

The study was supported by the RFBR Grants nos. 08–02–97039 and 09–02–91071.

References

[1] Korotkov AS, Slavinsky MM, Sutin AM. Nonlinear vibro-acoustic method for diagnostics of metal strength properties. In: Hobaek, H, editor. Proceedings of 13th ISNA. Advances in nonlinear acoustics. Singapore–New Jersey–London–Hong Kong: World Scientific; 1993. p. 370–5.
[2] Korotkov AS, Sutin AM. Modulation of ultrasound by vibrations in metal constructions with cracks. Acoust Lett 1994;18:59–62.
[3] Nagy PB. Fatigue damage assessment by nonlinear ultrasonic materials characterization. Ultrasonics 1998;36(1–5):375–81.
[4] Ekimov AE, Didenkulov IN, Kazakov VV. Modulation of torsional waves in a rod with a crack. J Acoust Soc Am 1999;106(3–1):1289.
[5] Johnson P. The new wave in acoustic testing. Materials world. J Inst Materials 1999;7:544.
[6] Tsyfansky SL, Beresnevich VI. Non-linear vibration method for detection of fatigue cracks in aircraft wings. J Sound Vib 2000;236(1):49–60.
[7] Zaitsev VYu, Sas P. Nonlinear response of a weakly damaged metal sample: a dissipative mechanism of vibro-acoustic interaction. J Vib Control 2000;6:803–22.
[8] Donskoy D, Sutin A, Ekimov A. Nonlinear acoustic interaction on contact interfaces and its use for nondestructive testing. NDT&E Int 2001;34:231–8.
[9] Van Den Abeele KEA, Sutin A, Carmeliet J, Johnson P. Microdamage diagnostics using nonlinear wave spectroscopy (NEWS). NDT&E Int 2001;34:239–48.
[10] Solodov I, Wackerl J, Pfleiderer K, Busse G. Nonlinear self-modulation and subharmonic acoustic spectroscopy for damage detection and location. Appl Phys Lett 2004;84:5386.
[11] Sutin AM, Johnson PA. Nonlinear elastic wave NDE II. Nonlinear wave modulation spectroscopy and nonlinear time reversed acoustics. In: Proceedings of 31st annual review of progress in QNDE. Proceedings of AIP Conference, vol. 760, 2005. p. 385–92.
[12] Rudenko OV. Giant nonlinearities in structurally inhomogeneous media and the fundamentals of nonlinear acoustic diagnostic techniques. Physics-Uspekhi 2006;49(1):69–87.
[13] Duffour P, Morbidini M, Cawley P. A study of the vibro-acoustic modulation technique for the detection of cracks in metals. J Acoust Soc Am 2006;119(3):1463–75.
[14] Straka L, Yagodzinskyy Yu, Landa M, Hänninen H. Detection of structural damage of aluminium alloy 6082 using elastic wave modulation spectroscopy. NDT&E Int 2008;41:554–63.
[15] Kittel C. Introduction to solid state physics. 7th ed. New York: Wiley; 1996.
[16] Matveyev AL, Nazarov VE, Zaitsev VYu, Potapov AI, Erilin ES, Sorokin SV, et al. Nonlinear acoustic method of crack detection in railway wheel pairs. World Nondestructive Testing 2004;4(26):65–8 [in Russian].
[17] Rudenko OV, Soluyan SI. Theoretical foundations of nonlinear acoustics. New York: Consultants Bureau; 1977.
[18] Naugolnykh K, Ostrovsky L. Nonlinear wave processes in acoustics. New York: Cambridge University Press; 1998.
[19] Salawu OS. Detection of structural damage through changes in frequency: a review. Eng Struct 1997;19(9):718–23.

[20] Zaitsev V, Sas P. Elastic moduli and dissipative properties of microinhomogeneous solids with isotropically oriented defects. Acustica-Acta Acustica 2000;86:216–28.
[21] Zaitsev V, Sas P. Influence of high-compliance porosity on the variation of P-and S-wave velocities in dry and saturated rocks: comparison of model and experiments. Phys Mesomech 2004;7(1–2):37–46.
[22] Zaitsev V, Sas P. Determining properties of high compliance porosity by use of an effective medium model based on crack description in terms of their normal and shear compliance parameters, In: Proceedings of the first south hemisphere international symposium on rock mechanics. Perth: Australian Centre for Geomechanics; 2008. p. 12.
[23] Mavko GM, Nur A. The effect of nonelliptical cracks on the compressibility of rocks. J Geophys Res 1978;83(B9):4459–68.
[24] Walsh JB. The effect of cracks on Poisson's ratio. J Geophys Res 1965;70: 5249.
[25] O'Çonnell RJ, Budiansky B. Seismic velocities in dry and saturated cracked solids. J Geophys Res 1974;79:5412–26.
[26] Goldstein H. Classical mechanics. Cambridge, MA: Addison-Wesley; 1950.
[27] Lifshitz EM, Landau LD. Quantum mechanics: non-relativistic theory. vol. 3, London: Butterworth-Heinemann; 1981.
[28] Zaitsev V, Nazarov V, Gusev V, Castagnede B. Novel nonlinear-modulation acoustic technique for crack detection. NDT&E Int 2006;39(3): 184–94.
[29] Zaitsev VYu, Matveev LA, Matveyev AL, Arnold W. Cascade cross modulation due to the nonlinear interaction of elastic waves in samples with cracks. Acoust Phys 2008;54:398–406.